

Exploring the potential of 3'-*O*-carboxy esters of thymidine as inhibitors of ribonuclease A and angiogenin

Kalyan S. Ghosh, Joy Debnath, Palash Dutta, Bijaya K. Sahoo and Swagata Dasgupta*

Department of Chemistry, Indian Institute of Technology, Kharagpur 721302, India

Received 13 October 2007; revised 2 January 2008; accepted 4 January 2008

Available online 10 January 2008

Abstract—In this study, compounds with a carboxy ester in lieu of the phosphate ester at the 3'-position have been employed to inhibit the ribonucleolytic activity of ribonuclease A (RNase A). Phosphates at the 3'-position of pyrimidine bases are well-known inhibitors of the protein. We have investigated the inhibition of RNase A by 3'-*O*-carboxy esters of thymidine. The compounds behave as competitive inhibitors with inhibition constants ranging from 42 to 95 μM . The mode of inhibition has also been confirmed by ^1H NMR studies of the active site histidines of RNase A. Docking studies have further substantiated the experimental results. The compounds are also found to inhibit the ribonucleolytic activity of angiogenin, a homologous protein and potent inducer of blood vessel formation.

© 2008 Elsevier Ltd. All rights reserved.

1. Introduction

Inhibitors of mammalian ribonucleases (RNases) that cleave ribonucleic acid (RNA) have often been utilized to limit the undesirable biological function of many ribonuclease type proteins. Several RNase homologs, including angiogenin,¹ eosinophil-derived neurotoxin (EDN),² and bovine seminal RNase A³, utilize their ribonucleolytic activities to bring forth effectual physiological effects, which are oftentimes related to certain disease processes.⁴ Apparently, to exhibit the angiogenic activity (growth of new blood vessels) of angiogenin its ribonucleolytic activity is essential, even though it is of lower magnitude ($\sim 10^5$ lower) than bovine pancreatic ribonuclease A (RNase A).⁵ Thus inhibitors of these proteins may be considered as potential lead compounds for the development of drug candidates.

The active site of RNase A, a convenient model system of this superfamily, is conventionally described in terms of multiple subsites for binding phosphate, base, and ribose moieties of the RNA substrate.^{6,7} The phosphate binding subsite of RNase A where phosphodiester bond cleavage occurs is designated as P₁, which contains the catalytic residues His 12, Lys 41, and His 119. Similarly

the ribonucleolytic site of angiogenin, which is identical to RNase A, is comprised of His 13, Lys 40, and His 114.⁸ A comparative schematic diagram of the nucleotide binding site of RNase A and angiogenin is given in Figure 1. The active site homology may be exploited by targeting RNase A as a suitable model to help the design of antiangiogenic compounds.

Many nucleoside and nucleotide-based small molecule inhibitors of ribonucleases have been identified.^{9,10} These nucleotide-based inhibitors have close resemblance to the natural substrate of RNase A and thus act as substrate mimics. Most of them are derivatized with the phosphate ester with an adenosine 5'-pyrophosphate derivative, pdUppA-3'-p being the most potent inhibitor known.¹¹ Replacement of the phosphate esters by 3'-amino groups proved to be a successful venture which has already been published in this journal.¹² The crystal structure of the complex of 3'-*N*-piperidine-4-carboxyl-3'-deoxy-*ara*-uridine with RNase A was also subsequently reported in this journal. The structure confirmed the interaction with active site residues despite the absence of the phosphate group.¹³ We have also reported the inhibition of RNase A with the major green tea polyphenols, that act as a noncompetitive inhibitors.^{14,15} These compounds show distinctly different behavior than the compounds reported here. This study has also been followed by the inhibition of RNase A by copper complexes of the two gallate containing polyphenols present in green tea.¹⁶

Keywords: Ribonuclease A; Angiogenin; Thymidine-3'-*O*-carboxy ester; Competitive inhibition; FT-IR; Circular dichroism; Docking.

* Corresponding author. Tel.: +91 3222 283306; fax: +91 3222 255303; e-mail: swagata@chem.iitkgp.ernet.in

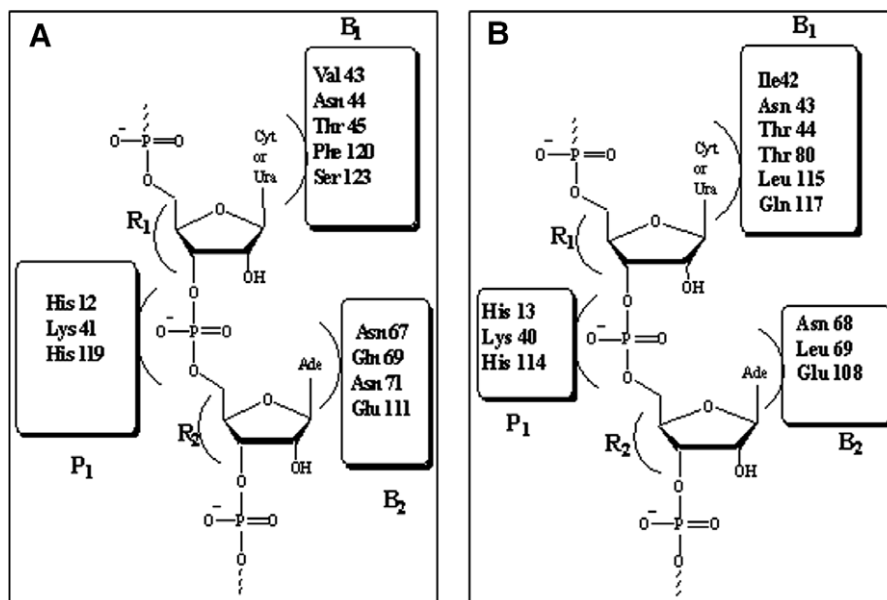


Figure 1. Key residues of active site of (A) RNase A and (B) human angiogenin.

In this study, the phosphate group at the 3'-position has been substituted with a carboxylate ester group. It might be assumed that the negative charge center on the carbonyl oxygen atom of the ester moiety would be able to perturb the ionic environment of the active site by interacting with protonated histidine or lysine residues. It is known that the pK_a values of histidine residues of the P_1 subsite change from 5.22/6.78 for free enzyme to 6.30/8.10 for the enzyme–substrate complex.¹⁷ A perturbation in the active site area would, therefore, be capable of disrupting the catalytic activity, which would tantamount to inhibition of the enzyme. The compounds synthesized have been shown to inhibit the ribonucleolytic activity of RNase A both qualitatively and quantitatively. Changes in the local pK_a of the active site histidines His 12 and His 119 were also determined. FT-IR and CD studies were used to monitor secondary structural changes occurring due to the interaction of the compounds with RNase A. Furthermore, this study is pertinent since these compounds would be expected to serve as potent inhibitors of the ribonucleolytic activity of angiogenin that in turn is expected to affect its angiogenic activity.⁵

2. Results and discussion

In this study we have checked the inhibition of RNase A by 3'-*O*-carboxy ester modified thymidines compared to 3'-TMP and 3'-CMP, reported inhibitors of RNase A.⁹ The inhibition of the ribonucleolytic activity of RNase A was initially checked by an agarose gel-based assay, where the degradation of tRNA by RNase A was monitored with and without the compounds (Fig. 2A). The most intense band observed in lane 1 is due to the presence of the control tRNA. The faint intensity of the band in lane 2 is due to the degradation of tRNA by RNase A. The differential intensity of the bands in lanes 3, 4, 5, and 6 qualitatively indicates the degree of RNase

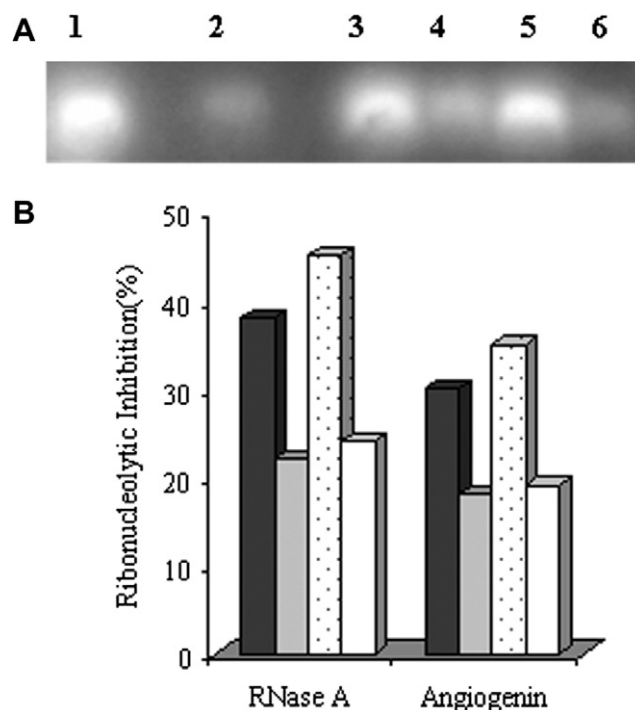


Figure 2. (A) Agarose gel-based assay for the inhibition of RNase A. Lane 1: tRNA; Lane 2: RNase A and tRNA; Lane 3: 0.6 mM compound 5, RNase A and tRNA; Lane 4: 0.6 mM compound 6, RNase A, and tRNA; Lane 5: 0.6 mM 3'-TMP, RNase A and tRNA; Lane 6: 0.6 mM 3'-CMP, RNase A, and tRNA. (B) Comparative ribonucleolytic inhibitory activities of RNase A and angiogenin by 5 (black) and 6 (gray) 3'-TMP (dotted) and 3'-CMP (white).

A inhibition by the synthesized compounds 5 and 6, 3'-TMP, and 3'-CMP, respectively. These results show that though the 3'-phosphate ester of thymidine is a better inhibitor, compounds 5 and 6 containing 3'-*O*-carboxylate esters also act as effective inhibitors of RNase A. We have also chosen 3'-CMP as a very well-known inhibitor of RNase A used as the standard inhibitor in our previ-

ous studies.^{12,14} Intensity observations qualitatively indicate that compound **5** is a more potent inhibitor than 3'-CMP whereas the extent of inhibition of **6** and 3'-CMP is comparable.

The inhibition of the ribonucleolytic activity of RNase A by **5** and **6** was further assessed quantitatively by precipitation assay. Considering identical concentrations (0.22 mM) for the compounds, we find that **5** and **6** inhibit RNase A by 38% and 22%, respectively, whereas with 3'-TMP and 3'-CMP the inhibition is 45% and 24%, respectively (Fig. 2B). The concentrations of compounds **5** and **6** at which 50% inhibition of RNase A occurs (IC_{50}), are 197 and 341 μ M, respectively (IC_{50} for 3'-TMP and 3'-CMP are 167 and 312 μ M, respectively). To further determine the nature of inhibition and the inhibition constants, kinetic experiments were conducted. The inhibition constant values obtained for **5** and **6** were 42 ± 1 and 95 ± 3 μ M, respectively. Eadie–Hofstee plots (Fig. 3) indicate that these two compounds behave as competitive inhibitors (convergence on the y-axis). The reported K_i values for 3'-TMP and 3'-CMP are 13.2 and 103 μ M.¹⁸ This indicates that compound **5** is a better inhibitor than 3'-CMP whereas compound **6** is comparable to 3'-CMP, however 3'-TMP is a better

inhibitor than both **5** and **6**. The order of inhibition constant values obtained for **5** and **6** correlates well with the results obtained from the agarose gel and precipitation assays.

Competitive inhibition of an enzyme is suggestive of a direct interaction of the inhibitors with the active site residues. In the reported hydrolytic mechanism of RNase A, in the transphosphorylation step, His 12 acts as a general base to deprotonate the 2'-oxygen atom of the substrate, which then attacks the phosphorus atom to form a pentavalent transition state.^{7,10,19} This species, which is stabilized by Lys 41, collapses to yield the cyclic 2',3'-phosphate intermediate. His 119 serves as a general acid to protonate the oxygen atom of the leaving group. This mechanism was confirmed by site-directed mutagenesis studies.^{19–21} Considering the acid–base role of the active site histidines, one can follow the pK_a changes

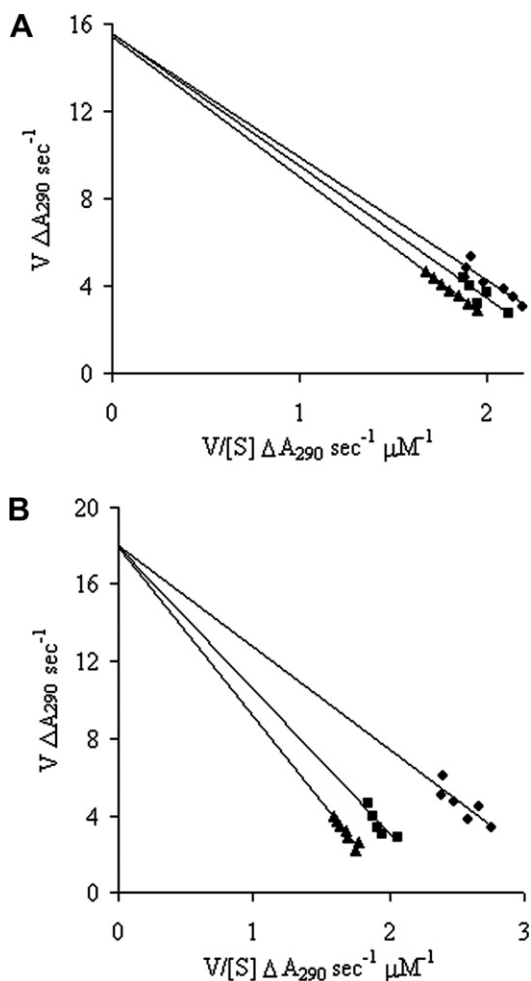


Figure 3. Eadie–Hofstee plot for inhibition of RNase A by (A) compound **5**: 6.7 μ M (▲), 3.3 μ M (■), and 0 μ M (●); (B) compound **6**: 62 μ M (▲), 30 μ M (■), and 0 μ M (●).

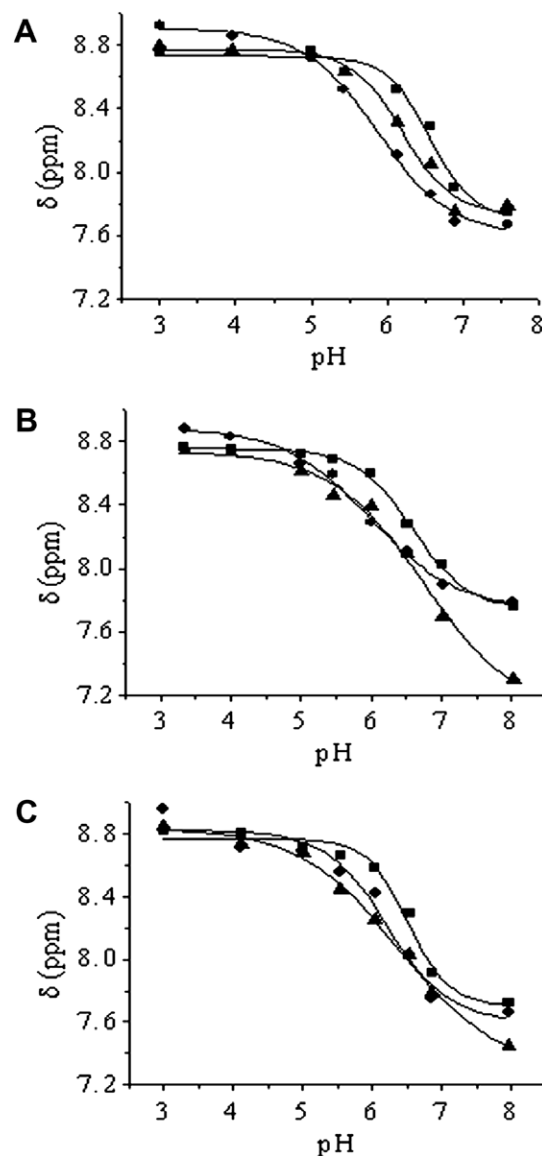


Figure 4. pH dependence of the histidine C-2 proton signals of (A) only RNase A, (B) RNase A with compound **5**, and (C) RNase A with compound **6**. Chemical shifts are shown for histidine residues His 12 (●), His 105 (■), His 119 (▲).

in the presence of inhibitors to monitor their behavior. From the ^1H NMR titration curve of the histidine C-2 proton (Fig. 4A), the observed $\text{p}K_{\text{a}}$ values for His 12, His 105, and His 119 are 5.88, 6.59, and 6.22, respectively, for free RNase A. When compound **5** and **6** complex with RNase A (Fig. 4B and C, respectively), the $\text{p}K_{\text{a}}$ values shift to 6.01, 6.62 and 6.77 for compound **5** and 6.23, 6.53, and 6.39 for compound **6**, respectively. Perturbation of the $\text{p}K_{\text{a}}$ values of His 12 and His 119 indicate that compounds **5** and **6** go to the active site of RNase A. We observe that the $\text{p}K_{\text{a}}$ values for His 105 remain practically unaltered (<1%) which is also similar to the reported change of $\text{p}K_{\text{a}}$ for His 105 in case of 2'-CMP²² and 3'-CMP.²³ The $\text{p}K_{\text{a}}$ value for His 119 shifts by $\sim 9\%$ in the presence of compound **5**. The increase in the $\text{p}K_{\text{a}}$ value indicates that the presence of the negative charge center has a direct influence on the environment of the imidazole ring of His 119. An increase in $\text{p}K_{\text{a}}$ is also observed when the negatively charged phosphate group interacts with the His residues for complexes with both 2'-CMP²² and 3'-CMP.²³ In the case of phosphate esters, however, there is a substantial change ($\sim 28\%$). This can be attributed to the formation of the dianion that is capable of perturbing the environment to a higher degree than compound **5** or **6**, where only a negatively polarized charge center on the carbonyl oxygen is resident. Interestingly, the $\text{p}K_{\text{a}}$ of histidines are unaffected in the cytidine–RNase A complex,²² where such interactions of the phosphate dianion with the His residues are absent. Our results thus indicate that the inhibition of RNase A by compound **5** is primarily because of its interaction with His 119. In case of compound **6**, relatively minor changes are observed for His 12 ($\sim 6\%$) and His 119 ($\sim 3\%$). The presence of the phenyl ring in this case could interact with Phe 120 resulting in a smaller perturbation to the His residues but nevertheless occupying the active site. The abstraction of the proton from 2'-OH by His 12 (acting as base) for cytidine phosphates is not also possible for compound **5** or **6**, which has no 2'-OH that explains the much lower $\Delta\text{p}K_{\text{a}}$ observed for the 3'-O-carboxy esters. The preferred docking poses for both the compounds are consistent with these changes in $\text{p}K_{\text{a}}$ (discussed later).

The effect of binding of these compounds on the overall secondary structure of RNase A was also investigated by FT-IR and CD spectroscopy. In FT-IR spectroscopy, amide I bands at 1645–1650 cm^{-1} (mainly C=O stretching) and the amide II band at 1548–1560 cm^{-1} (C–N stretching coupled with an N–H bending mode) of proteins change on interaction with small molecules and ligands.²⁴ The fitted Gaussian curves in the amide I region with spectral ranges from 1610 to 1632 cm^{-1} , 1636 to 1644 cm^{-1} , 1650 to 1662 cm^{-1} , and 1665 to 1680 cm^{-1} are attributed to the β -sheet, random coil, α -helix and turn structures, respectively.^{25,26} Changes in the peak positions of the amide I and II bands in the FT-IR spectra of RNase A are observed with both compounds. This is visible in the difference spectra (Fig. 5). With compound **5** at a protein ligand ratio of 1:1 the peaks at 1663, 1643, and 1629 cm^{-1} indicate changes in α -helix, random structure, and β -sheet con-

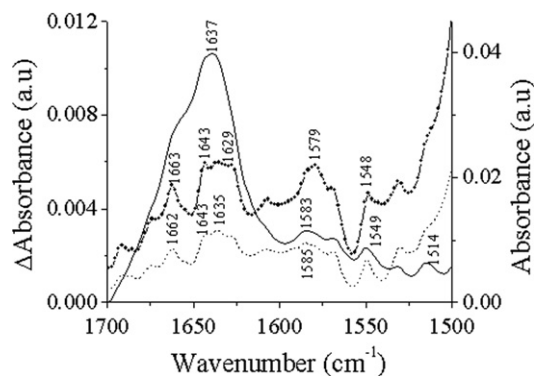


Figure 5. FT-IR difference spectra of RNase A complexes with compound **5** (—•—) and compound **6** (···) at RNase A:ligand as 1:1 (left hand axis) with FT-IR spectra of free RNase A (—) (right hand axis).

tents, respectively. Similarly for compound **6** at the same protein ligand ratio, difference spectra reflect changes in α -helix (1662 cm^{-1}), random structure (1643 cm^{-1}), and β -sheet (1635 cm^{-1}) content. The increase in intensity observed in the difference spectra between 1549 and 1548 cm^{-1} in the amide II region for compounds **5** and **6**, respectively, can be attributed to the interaction of the compounds with the backbone of the protein. The distinctive changes in the content of secondary structural elements are more prominent in the deconvoluted spectra of RNase A and its complexes with compounds **5** and **6** (Fig. 6).

CD spectroscopic studies of free RNase A and its complexes with compounds **5** and **6** also indicate a perturbation in the secondary structure (Fig. 7). The percentage of secondary structural elements for RNase A and its complexes with compounds **5** and **6** at 1:0.5 and 1:1 ratios was determined using SELCON3 method in DICHROWEB.²⁷ We find that there is an increase in the α -helix content ($\sim 9\%$) with a concomitant reduction in random ($\sim 5\%$) and turn structures ($\sim 4\%$) for complexation with compound **5** at the higher ratio. An increase in α -helix content of RNase A has also been observed with the nucleoside 3-azido-3-deoxythymidine (AZT).²⁸ In case of compound **6** at the higher ratio, minor increases in both the α -helix and β -sheet contents ($\sim 6\%$ and 4% , respectively) are indicative more of conformational adjustments on complex formation rather than a major change in secondary structure. This was compensated by a decrease in the content of random structure by $\sim 10\%$. The stabilization of β -sheet conformation of RNase A has also been observed in the interaction of RNase A with (–)-epigallocatechin.¹⁵

Protein–ligand docking studies were performed to obtain some insight into the amino acid residues of RNase A involved in interactions with compounds **5** and **6**. Though the crystal structure of the complex can represent specific details of the interactions, general observations may be obtained from docking studies. Our earlier studies¹³ with another synthetic inhibitor of RNase A revealed that docking poses are similar to those obtained from structural studies (RMSD 0.47 Å). Interest-

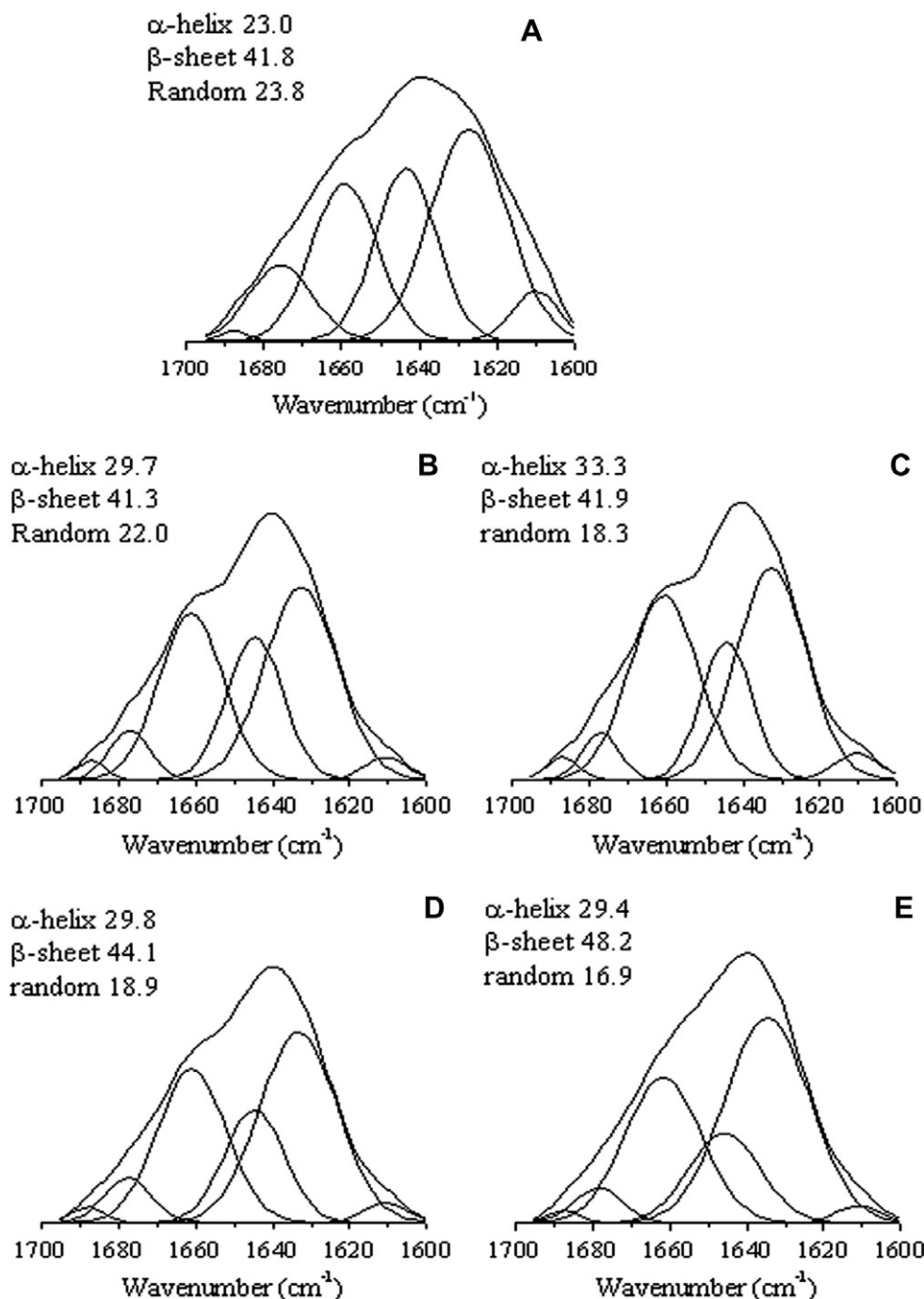


Figure 6. Deconvoluted spectra of RNase A and its complexes with compound **5** and **6**: (A) RNase A, (B) RNase A-compound **5** (1:0.5), (C) RNase A-compound **5** (1:1), (D) RNase A-compound **6** (1:0.5), and (E) RNase A-compound **6** (1:1). The percentage of α -helix, β -sheet and random coil is indicated in the legends.

ingly, that inhibitor was also competitive in nature and was found to dock to the active site, which was further confirmed by structural studies (PDB entry 2G8R). In the docking experiments for **5** and **6** with RNase A we also observe a competitive mode of binding, which correlates well with the experimental studies. The docking pose shown in Figure 8A (for compound **5**) reveals that the ester carbonyl oxygen is 2.72 Å away from the N δ 1 atom of His 119 and the distance between the O atom at the 3' position of compound **5** and N ϵ 2 of His 12 is

2.72 Å. In Figure 8B, compound **6** is close to Gln 11, which is very close to His 12. The presence of the compound **6** in the proximity of His 12 may result in the perturbation of the pK_a of this residue as opposed to His 119 for compound **5**. To compare with the mode of inhibition of 3'-TMP and 3'-CMP with our compounds, we have also performed the docking of these two monophosphates with RNase A (Fig. 8C and D, respectively). In this case we find that the phosphate dianion is within hydrogen bonding distance of both His 12 and His 119,

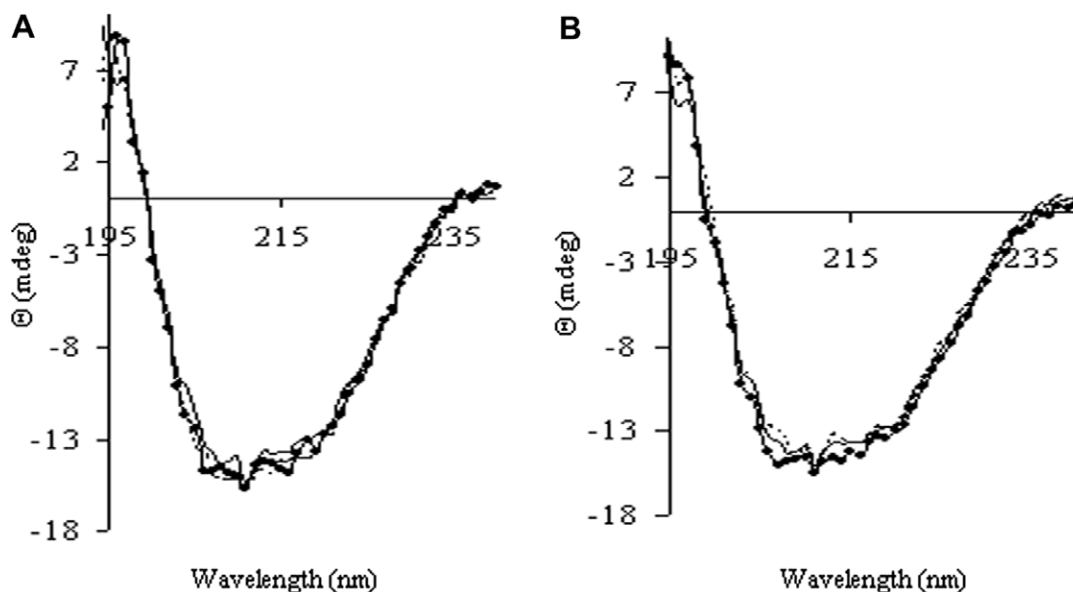


Figure 7. CD spectra of (A) RNase A-compounds **5** and (B) RNase A-compound **6** complexes. Free RNase A (—), RNase A:ligand 1:0.5 (.....), and RNase A:ligand 1:1 (---●---).

as expected. This is also reflected in the increase of pK_a of both the histidines when complexed with 3'-CMP.²³ In this context we can compare the docking of compounds **5** and **6** with the previously reported 3'-non-phosphate inhibitor (3'-*N*-piperidine-4-carboxyl-3'-deoxy-*ara*-uridine)¹³ where the 4-carboxypiperidine moiety of the inhibitor molecule binds at the subsite B₁ by hydrogen bonding interactions using its carboxyl group with Thr 45. The uracyl group binds through hydrogen bond interactions with the side chains His 119 and Asp 121. For this compound the nucleobase interacts with P₁ subsite residues, whereas for compound **5** the ester carbonyl oxygen and for compound **6** the 5'-oxygen of the ribose ring appear to interact with the active site.

An extension of the docking study to obtain the structure–activity relationship between the carboxy esters of different nucleobases with their inhibition potency for RNase A was also carried out. In this study, results of which are given in the [Supplementary material](#), we have compared the docking modes of 3'-*O*-acetyl and 3'-*O*-benzoyl esters of three deoxypyrimidines with estimates of their K_i values ([Table S1](#)). In brief, we found that the 3'-*O*-acetyl ester of thymidine was found to be a better inhibitor than the corresponding cytidine analogue, whereas the uridine analogue was almost comparable to thymidine. However, for the 3'-*O*-benzoyl esters the inhibition follows the order U > T > C. Altering the position of the carboxyester with the same nucleobase (in this case thymidine), the 3'-*O*-esters show better inhibition than the corresponding 5'-*O*-esters. Finally we have looked at the inhibition potency of 2'-deoxy-3'-phosphate of three pyrimidines and compared this with the respective 3'-*O*-esters. This also indicated that the thymidine phosphate was best amongst three. The inhibition constant of 3'-*O*-acetyl ester was com-

parable with that of 3'-phosphate of thymidine, whereas that of 3'-*O*-benzoyl ester was lower. The docking poses for these compounds are given in [Supplementary Information](#).

Since both compounds **5** and **6** inhibited the ribonucleolytic activity of RNase A, the next step was to check whether these carboxylate esters were capable of inhibiting the ribonucleolytic activity of angiogenin. In the precipitation assay as described in [Section 3.4](#), for monitoring the inhibition of the ribonucleolytic activity of angiogenin ([Fig. 2B](#)), we observed that compounds **5** and **6** inhibit 30% and 18% of the enzymatic activity, respectively. The corresponding inhibition with 3'-TMP and 3'-CMP is 19% and 35%. The concentrations of compound **5** and **6** at which 50% inhibition of ribonucleolytic activity of angiogenin occurs (IC_{50}) are 250 and 417 μ M, respectively (IC_{50} for 3'-TMP and 3'-CMP are 214 and 395 μ M, respectively). According to one of our earlier studies, this implies that the angiogenic activity should also be affected due to the disruption in the enzymatic activity.¹² A clearer understanding of the mechanism or mode of binding is underway to assess how these compounds may be better modified to provide more potent inhibition.

3. Materials and methods

3.1. Materials

RNase A, yeast tRNA, 2',3'-cCMP, 3'-CMP, 3'-TMP, human angiogenin, and human serum albumin were from Sigma–Aldrich. All other reagents were from SRL India. UV measurements were made using a Perkin Elmer UV–vis spectrophotometer (Model Lambda 25). Concentrations were determined using the follow-

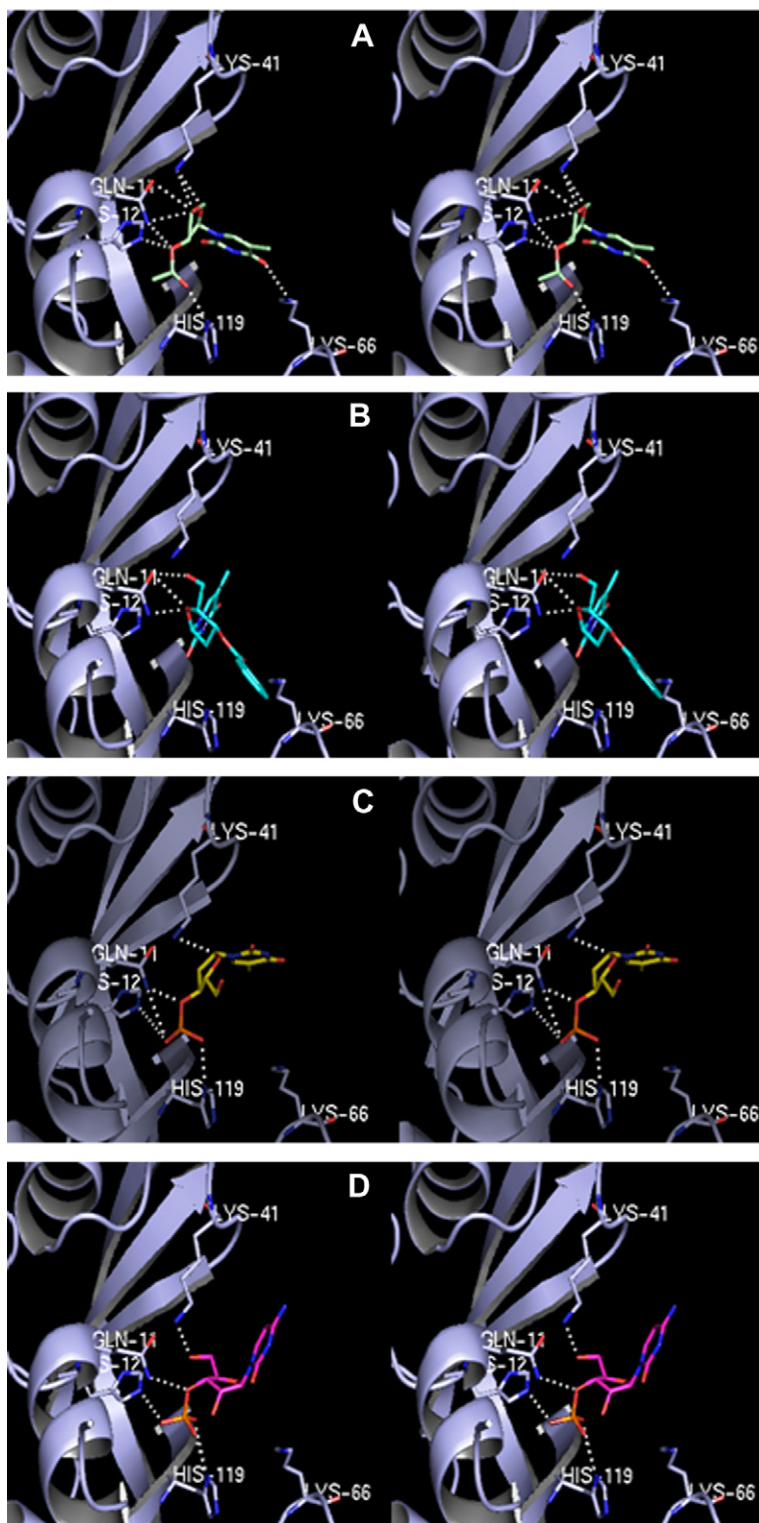
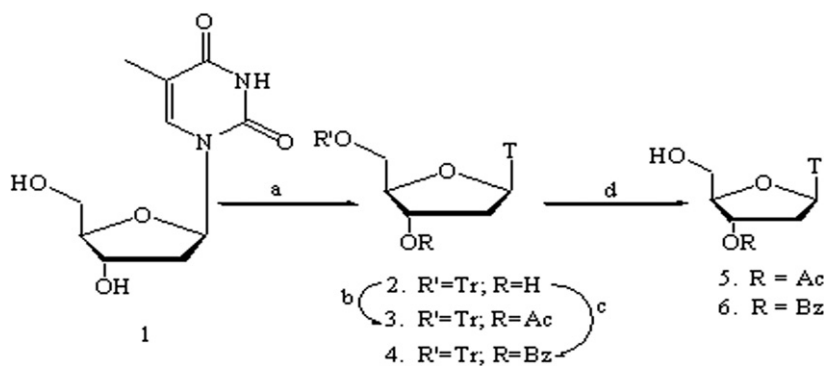


Figure 8. Stereoview of the docked conformations of (A) compound **5**, (B) compound **6**, (C) 3'-TMP, and (D) 3'-CMP with ribonuclease A. The protein conformations have been kept identical for comparison. His 12, Lys 41, and His 119 have been marked to indicate the location of the catalytic site. Possible hydrogen bonds are shown as dashed lines.

ing spectral data: RNase A $\epsilon_{278.5} = 9800 \text{ M}^{-1} \text{ cm}^{-1}$,²⁹ 2',3'-cCMP $\epsilon_{268} = 8500 \text{ M}^{-1} \text{ cm}^{-1}$, and ¹⁸ 3'-CMP $\epsilon_{260} = 7600 \text{ M}^{-1} \text{ cm}^{-1}$,³⁰ respectively. The stock solutions of compounds **5** and **6** were prepared in ethanol and diluted prior to use maintaining a maximum alco-

hol concentration less than 3% in the following studies. The extinction coefficients of compounds **5** and **6** at 266 nm were determined and their concentrations were measured using $\epsilon_{266} = 5950$ and $6355 \text{ M}^{-1} \text{ cm}^{-1}$, respectively.



Scheme 1. Synthetic scheme for the synthesis of 3'-*O*-carboxy esters of thymidine. Reagents and conditions: (a) TrCl/py, rt, 48 h; 92%; (b) Ac₂O/Py, rt, 12 h; 95%; (c) BzCl/Py/DCM, rt, 2–3 h; 88%; (d) TFA/DCM (1:4); 75% for **5** and 70% for **6**.

3.2. Synthesis of 3'-*O*-carboxy esters of thymidine

The 3'-*O*-carboxy esters were synthesized starting from thymidine according to a general synthetic procedure as described by Zhou et al.³¹ (Scheme 1). In brief compound **1** (3.6 mmol) was tritylated by stirring with trityl chloride (5.4 mmol) in pyridine for two days to obtain compound **2**. Compound **3** was obtained by treating **2** (4.3 mmol) with acetic anhydride (4.3 mmol) in dry pyridine for 12 h at room temperature. Compound **4** was obtained by treating **2** (4.1 mmol) with benzoyl chloride (4.1 mmol) for 2–3 h at room temperature. Then detritylation of **3** and **4** was performed with 20% trifluoroacetic acid in dichloromethane to achieve the target molecules **5** and **6**.

3.2.1. Compound 5. Yield: 75%, ¹H NMR (CDCl₃) (400 MHz): δ 8.39 (br s, 1H); 7.50 (s, 1H); 6.25 (t, *J* = 7.2 Hz, 1H); 5.35 (m, 1H); 4.09 (m, 1H); 3.93 (m, 2H); 2.41 (m, 2H); 2.10 (s, 3H); 1.92 (s, 3H); ¹³C NMR (CDCl₃) (100 MHz): δ 170.7; 163.8; 150.5; 136.3; 111.3; 85.8; 85.0; 74.7; 62.5; 37.2; 20.9; 12.5; HRMS (ES+Na)⁺: Calculated for C₁₂H₁₆O₆N₂Na: 307.1341, found: 307.1347.

3.2.2. Compound 6. Yield: 70%, ¹H NMR (DMSO-*d*₆) (400 MHz): δ 8.01–7.52 (m, 5H); 7.78 (s, 1H); 6.28 (t, *J* = 7.2 Hz, 1H); 5.47 (m, 1H); 4.14 (m, 1H); 3.69 (m, 2H); 2.38 (m, 2H); 1.78 (s, 3H), ¹³C NMR (DMSO-*d*₆) (100 MHz): δ 165.6, 164.1, 150.9; 136.3, 134.0, 129.7 (2C); 129.2 (3C); 110.2; 84.9, 84.2; 76.1; 61.8; 37.0; 12.7; HRMS (ES+Na)⁺: Calculated for C₁₇H₁₈O₆N₂Na: 369.1873, found: 369.1869.

3.3. Agarose gel-based assay

Inhibition of RNase A by **5** and **6** was checked qualitatively by the degradation of tRNA in an agarose gel. In this method, 20 μl of RNase A (0.66 μM) was mixed with 20 μl each of 1.5 mM **5**, **6**, 3'-TMP or 3'-CMP solutions to a final volume of 50 μl and incubated for 6 h. Twenty microliter aliquots of the incubated mixtures were then mixed with 20 μl of tRNA solution (5.0 mg/ml tRNA, freshly dissolved in RNase free water) and incubated for another 30 min. Ten microliters of sample buffer which contains 10% glycerol and 0.025% bromo-

phenol blue was added to the mixture. Twenty microliters from each solution was extracted and loaded onto a 1.1% agarose gel. The undegraded tRNA was visualized by ethidium bromide staining under UV light.

3.4. Precipitation assay

The effect of **5** and **6** on the ribonucleolytic activity of the RNase A and angiogenin was examined with yeast tRNA as the substrate as described by Bond.³² Five microliters of 0.2 μM RNase A and 0.2 μM angiogenin and their incubated mixtures with 10 μl of **5** (225 μM), **6** (225 μM), 3'-TMP (225 μM), and 3'-CMP (225 μM) each were added separately to the assay mixture containing 0.1 mg of yeast tRNA in 0.1 M Tris–HCl buffer having pH 7.5, 5 mM EDTA, and 10 μg HSA in a final volume of 50 μl. For RNase A after incubation of the reaction mixture at 37 °C for 30 min and for angiogenin after incubation for 4 h, 100 μl of ice-cold 1.14 N perchloric acid containing 6 mM uranyl acetate was added to quench the reaction. The solution was then kept in ice for another 30 min and centrifuged at 4 °C for 5 min. Hundred microliters of the supernatant was taken and diluted to 500 μl. The change in absorbance at 260 nm was measured and compared to a control set.

3.5. Inhibition kinetics

The inhibition of RNase A by **5** and **6** was assessed individually by a spectrophotometric method as described by Anderson et al.¹⁸ The assay was performed in oligo vinylsulfonic acid free³³ 0.1 M Mes–NaOH buffer, pH 6.0, containing 0.1 M NaCl using 2',3'-cCMP as the substrate. For **5**, the substrate concentrations ranged from 0.14 to 0.28 mM and the inhibitor concentrations ranged from 0 to 6.7 μM. For **6**, the substrate concentrations varied from 0.13 to 0.25 mM and inhibitor concentrations were from 0 to 62 μM. The RNase A concentration used was 10 μM. The inhibition constants were determined from initial velocity data using an Eadie–Hofstee plot, where *V* versus *V*/[*S*] is plotted to obtain the kinetic constants according to the following equation:

$$V = \frac{-K_s V}{[S]} + V_{\max} \quad \text{where } K_s = K_m \left(1 + \frac{[I]}{K_i} \right)$$

V is the initial velocity, $[S]$ is the substrate concentration, $[I]$ is the inhibitor concentration, K_m is the Michaelis constant, K_i is the inhibition constant and V_{max} is the maximum velocity. From the slopes of the lines (K_s), the inhibition constants were calculated for both the compounds.

3.6. Proton NMR study

Exchangeable hydrogen atoms of RNase A were replaced by deuterium to facilitate the pH titration by ^1H NMR. To exchange hydrogen by deuterium the protein was dissolved in D_2O incubated at 50°C for 20 min, and then lyophilized.³⁴ This was repeated thrice. The lyophilized protein was then dissolved in D_2O containing 0.2 M NaCl. Afterward DCl and NaOD solutions were used to adjust the pH^* for the range 3–8, where pH^* is the direct measure of the pH which was not corrected for a deuterium isotope effect at 30°C . The [ligand]/[enzyme] molar ratio was 5:1, which was maintained for both compounds **5** and **6**. ^1H NMR data were recorded on Bruker 400 MHz spectrometer at 22.5°C . The acquisition time was 2 s with 100 scans. The observed δ value was recorded with respect to sodium 2,2-dimethyl-2-silapentane 5-sulfonate (DSS). The values of δ_{obs} for histidine C-2 protons at different pH were fitted to a least square sigmoidal curve.

3.7. FT-IR studies

RNase A (16 mg/ml) was dissolved in 20 mM phosphate buffer of pD 7.2 in 99.9% D_2O . RNase A: ligand ratios of 1:0.5 and 1:1 were prepared for the both compounds **5** and **6**. FT-IR measurements were carried out at 25°C on a Nexus-870 FT-IR spectrometer (Thermo Nicolet Corporation) equipped with a germanium-attenuated total reflection (ATR) accessory, a DTGS KBr detector, and a KBr beam splitter. All spectra were taken via the attenuated total reflection (ATR) method with a resolution of 4 cm^{-1} , with 256 scans each. Control buffer spectra (20 mM phosphate buffer of pD 7.2) were also recorded under identical conditions. The background was corrected before every sample.

IR spectra obtained were determined following the method of Byler and Susi.²⁴ The relative amounts of secondary structural elements of RNase A and the RNase A complexes with compounds **5** and **6** were processed by analyzing the area under the Gaussian curve. Each Gaussian band is assigned to a secondary structure according to the frequency of its maximum: α -helix ($1650\text{--}1662\text{ cm}^{-1}$), β -sheet ($1610\text{--}1632\text{ cm}^{-1}$), random coil ($1636\text{--}1644\text{ cm}^{-1}$), turn ($1665\text{--}1680\text{ cm}^{-1}$), and β -anti-parallel ($1680\text{--}1692\text{ cm}^{-1}$).^{25,26} The areas of all the component bands assigned to a given conformation are then summed and divided by the total area. The number obtained is taken as the proportion of the polypeptide chain in that particular conformation.²⁴

3.8. Circular dichroism (CD) measurements

Circular dichroism measurements were made on a Jasco-810 CD spectrophotometer, using 2 mm path length

at 25°C . The spectra were recorded in the range of 190–240 nm with a scan rate of 50 nm/min and a response time of 4 s. For baseline correction, CD spectra of buffer (20 mM phosphate buffer of pH 7.0) containing variable concentrations of ligands were collected and were subtracted from each sample spectra. The RNase A concentration was $12.5\ \mu\text{M}$ and complex mixtures with RNase A: ligand ratios of 1:0.5 and 1:1 were analyzed. Results were expressed as Θ and secondary structures were determined using SELCON3 method (Reference set 7) in DICHROWEB,²⁷ an online server for protein secondary structure analyses from circular dichroism spectroscopic data.

3.9. Docking studies

The crystal structure of RNase A-3'-CMP complex (PDB entry 1RPF) was downloaded from the Protein Data Bank.³⁵ Protein and ligand (3'-CMP) structures were extracted individually from it. The 3D structures of the compounds were generated by Sybyl 6.92 (Tripos Inc., St. Louis, USA) and their energy-minimized conformations were obtained with the help of the MMFF94 force field using MMFF94 charges. The FlexX software as part of the Sybyl suite was used for docking of all the compounds to RNase A. PyMol³⁶ was used for visualization of the docked conformations.

The coordinates of the docked ligand molecules obtained from FlexX in Sybyl were used in AutoDock 3.0 to get an estimate of the inhibition constants (K_i).³⁷ Polar hydrogen atoms were added and Kollman United Atomic (KOLLUA) charges assigned to the protein. A grid size of $20 \times 20 \times 20\ \text{\AA}^3$ with a grid spacing of $0.425\ \text{\AA}$ was used keeping other default parameters. Ligand docking was carried out with the AutoDock 3.0.5 Lamarckian Genetic Algorithm (GA).³⁷ For all the ligands the inhibition constant (K_i) is estimated at 298.15 K. The root mean square deviation (RMSD) value for the ligand molecule over all the docked structures, obtained from Sybyl and AutoDock docking programs, varied between 0.40 and 0.92.

Acknowledgments

S.D.G. is grateful to the Department of Science and Technology (DST), Government of India for financial support (Grant No. SR/FTP/LS-A-06/2001). J.D. thanks CSIR, New Delhi, for a senior research fellowship. The authors are thankful to Prof. Tanmaya Pathak, Department of Chemistry, Indian Institute of Technology, Kharagpur, for helpful discussion and comments.

Supplementary data

Supplementary data associated with this article can be found, in the online version, at [doi:10.1016/j.bmc.2008.01.003](https://doi.org/10.1016/j.bmc.2008.01.003).

References and notes

1. Fett, J. W.; Strydom, D. J.; Lobb, R. R.; Alderman, E. M.; Bethune, J. L.; Riordan, J. F.; Vallee, B. L. *Biochemistry* **1985**, *20*, 5480.
2. Sorrentino, S.; Glitz, D. G.; Hamann, K. J.; Loegering, D. A.; Checkel, J. L.; Gleich, G. J. *J. Biol. Chem.* **1992**, *267*, 14859.
3. Matousek, J. *Comp. Biochem. Physiol. C* **2001**, *129*, 175.
4. Loverix, S.; Steyaert, J. *Curr. Med. Chem.* **2003**, *10*, 779.
5. Shapiro, R.; Riordan, J. F.; Vallee, B. L. *Biochemistry* **1986**, *25*, 3527.
6. Iwahashi, K.; Nakamura, K.; Mitsui, Y.; Ohgi, K.; Irie, M. *J. Biochem.* **1981**, *90*, 1685.
7. Nogue's, M. V.; Vilanova, M.; Cuchillo, C. M. *Biochim. Biophys. Acta* **1995**, *1253*, 16.
8. Russo, N.; Acharya, K. R.; Vallee, B. L.; Shapiro, R. *Proc. Natl. Acad. Sci. U.S.A.* **1996**, *93*, 804.
9. Russo, A.; Acharya, K. R.; Shapiro, R. *Methods Enzymol.* **2001**, *341*, 629.
10. Raines, R. T. *Chem. Rev.* **1998**, *98*, 1045.
11. Russo, N.; Shapiro, R. *J. Biol. Chem.* **1999**, *274*, 14902.
12. Maiti, T. K.; De, S.; Dasgupta, S.; Pathak, T. *Bioorg. Med. Chem.* **2006**, *14*, 1236.
13. Leonidas, D. D.; Maiti, T. K.; Samanta, A.; Dasgupta, S.; Pathak, T.; Zographos, S. E.; Oikonomakos, N. G. *Bioorg. Med. Chem.* **2006**, *14*, 6055.
14. Ghosh, K. S.; Maiti, T. K.; Dasgupta, S. *Biochem. Biophys. Res. Commun.* **2004**, *325*, 807.
15. Ghosh, K. S.; Maiti, T. K.; Debnath, J.; Dasgupta, S. *Proteins* **2007**, *69*, 566.
16. Ghosh, K. S.; Maiti, T. K.; Mandal, A.; Dasgupta, S. *FEBS Lett.* **2006**, *580*, 4703.
17. Herries, D. G.; Mathias, A. P.; Rabin, B. R. *Biochem. J.* **1962**, *85*, 127.
18. Anderson, D. G.; Hammes, G. G.; Walz, F. G. *Biochemistry* **1968**, *7*, 1637.
19. Thompson, J. E.; Raines, R. T. *J. Am. Chem. Soc.* **1994**, *116*, 5467.
20. Trautwein, K. P.; Holliger, P.; Stackhouse, J.; Benner, S. A. *FEBS Lett.* **1991**, *281*, 275.
21. Messmore, J. M.; Fuchs, D. N.; Raines, R. T. *J. Am. Chem. Soc.* **1995**, *117*, 8057.
22. Meadows, D. H.; Roberts, G. C. K.; Jardetzky, O. *J. Mol. Biol.* **1969**, *45*, 491.
23. Meadows, D. H.; Jardetzky, O. *Proc. Natl. Acad. Sci. U.S.A.* **1968**, *61*, 406.
24. Byler, D. M.; Susi, H. *Biopolymers* **1986**, *25*, 469.
25. Susi, H.; Byler, D. M. *Methods Enzymol.* **1986**, *130*, 290.
26. Dong, A. C.; Huang, P.; Caughey, W. S. *Biochemistry* **1990**, *29*, 3303.
27. Whitmore, L.; Wallace, B. A. *Nucleic Acids Res.* **2004**, *32*, W668.
28. Gaudreau, S.; Novetta-dellen, A.; Neault, J. F.; Diamantoglou, S.; Tajmir-riahi, H. A. *Biopolymers* **2003**, *72*, 435.
29. Sela, M.; Anfinsen, C. B. *Biochim. Biophys. Acta* **1957**, *24*, 229.
30. Bolen, D. W.; Flogel, M.; Biltonent, R. *Biochemistry* **1971**, *10*, 4136.
31. Zhou, W.; Upendran, S.; Roland, A.; Jin, Y.; Iyer, R. P. *Bioorg. Med. Chem. Lett.* **2000**, *10*, 1249.
32. Bond, M. D. *Anal. Biochem.* **1988**, *173*, 166.
33. Smith, B. D.; Soellner, M. B.; Raines, R. T. *J. Biol. Chem.* **2003**, *278*, 20934.
34. Quirk, D. J.; Raines, R. T. *Biophys. J.* **1999**, *76*, 1571.
35. Berman, H. M.; Westbrook, J.; Feng, Z.; Gilliland, G.; Bhat, T. N.; Weissig, H.; Shindyalov, I. N.; Bourne, P. E. *Nucleic Acids Res.* **2000**, *28*, 235.
36. DeLano, W. L. The PyMOL Molecular Graphics System, DeLano Scientific, San Carlos, CA, USA, 2006. <http://pymol.sourceforge.net/>.
37. Morris, G. M.; Goodsell, D. S.; Halliday, R. S.; Huey, R.; Hart, W. E.; Belew, R. K.; Olson, A. J. *J. Comput. Chem.* **1998**, *19*, 1639.